Casting Solutions for Readiness

Lube Free Die Casting

September 17, 2017

R. Allen Miller

Professor Emeritus, The Ohio State University

Abstract

Lubrication free die casting generally means that surface spray is eliminated which eliminates one of the tools used for control of the die temperature. The primary objective of this work was to explore the implications of loss of spray cooling and evaluate strategies for cooling design to compensate for this loss.

It was known at the start of the project that good, well-engineered, internal cooling can compensate for the loss of spray and field tests performed as part of the project confirmed this fact. Die cooling system design principles have long called for sufficient internal cooling to accommodate the full heat load that is imposed on the die and some casters achieve this objective with good design but many lack the understanding of heat transfer necessary to achieve the objective or prefer to use spray.

This work demonstrated several of the physical principles that control the die thermal response. A one-dimensional (1-D) model that combines numerical and analytical solution techniques was used to perform several sensitivity studies that help visualize the tradeoffs inherent when spray cooling is reduced or eliminated. The 1-D model results are simple enough to display graphically for easy understanding but complete enough to provide needed engineering insight.

Several strategies intended to compensate for the elimination of spray were considered including "do nothing and letting the die run hot," increase the cycle time, and intermittent spray where spray is applied but not every cycle. While these approaches work in some cases, internal cooling is shown to be more effective.

Analysis of the heat transfer characteristics of internal cooling lines produced design relationships that relate the required heat transfer and temperature change in the coolant with cooling line design parameters. Methods used previously did not account for the temperature rise in the coolant.

Most results of the work are in the form of simple, graphical explanations of the heat transfer phenomena that occur in die casting dies. The 1-D transient and spatial die temperature results illustrate the effects of cycle time, thermal mass, cooling line placement etc. NADCA has course materials for both die design and die thermal management that will benefit from the inclusion of material in this form. A preliminary revision of course EC 415, Thermal Design and Control, has been completed including some of the spatial and transient response examples from this work and including the cooling line design relationships. Finalization of the presentation materials and revisions of the text material will be completed by early 2018.

Much of this work is also relevant to general computer modelling issues. Simulations generally do not explicitly model cooling lines as heat exchangers and the quasi-equilibrium phenomenon is not well understood. Results from this research that include these topics are included in three new NADCA computer modeling webinars that will be presented for the first time in the fourth quarter of 2017.

Generally modelling results, and especially the quasi-equilibrium results, were presented at the 2016 NADCA Congress and are included in the transactions (Miller 2016).

Introduction and Background

Lubrication free die casting generally means that surface spray is eliminated which also eliminates one of the tools commonly used for control of the die temperature. The primary objective of this work was to explore the implications of loss of spray cooling and evaluate strategies for cooling design to compensate for this loss.

It was known at the start of the project that good, well-engineered, internal cooling can make up for the loss of spray and the field test completed as part of the project have confirmed this. Die cooling system design principles have long called for sufficient internal cooling to accommodate the full heat load that is imposed on the die and many casters achieve this objective with good design. Detailed cooling design is very much dependent on geometry details and it is not possible to construct a cooling system design in the abstract. It is, however, possible to illustrate some of the key tradeoffs and that was the focus of this work.

The geometry effects and cooling complexities due to geometry are evident in Figure 1. The figure illustrates the temperature of six test specimen castings at the time of ejection from the die. The individual specimen are of different dimensions and volumes and therefore create a difficult challenge to uniformly cool. The biscuit area at the bottom of the figure and the two larger specimen are roughly 100 – 125^{o}C hotter than the intermediate sized bars and more than 200^{o}C hotter than the smallest cross section bar located at the extreme left.

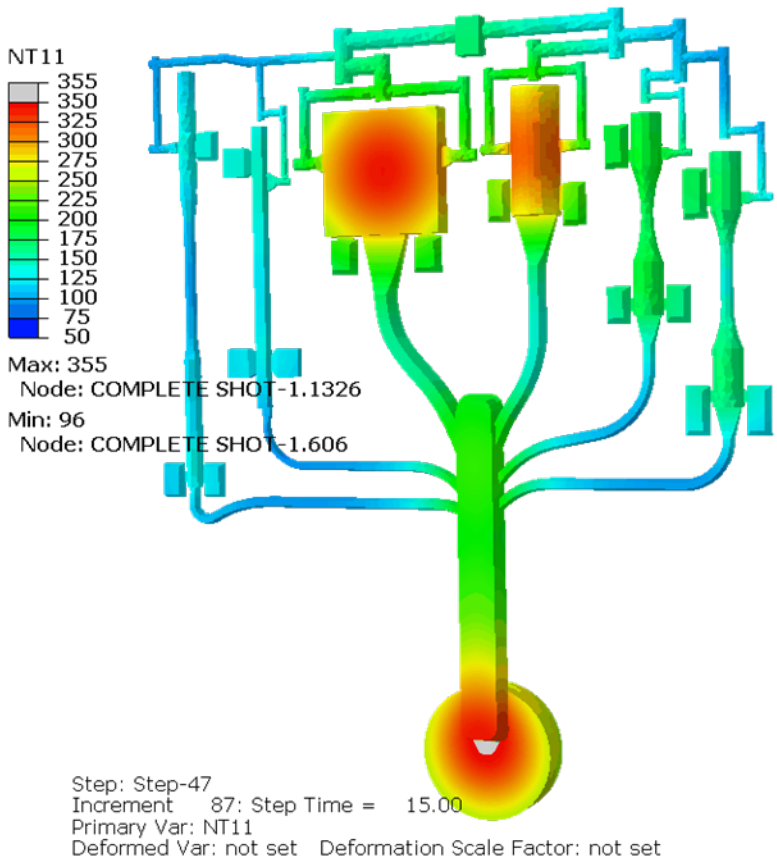

Figure 1 Example – Casting Temperature at Ejection

The moving and fixed sides of the die at the same point in the casting cycle are shown in Figure 2. The part and die temperatures are approximately the same at this point, a characteristic that will be explored more fully later in this report. The hot spots on the die surface are clearly visible. Figure 3 shows the surface temperature distribution immediately after spray.

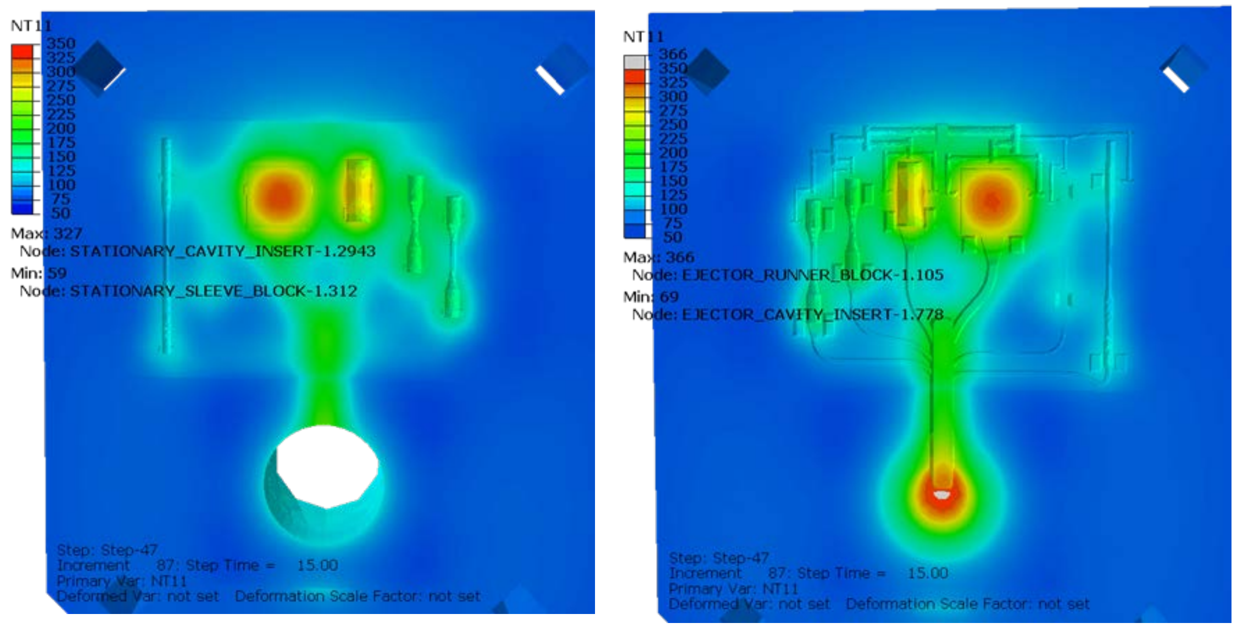

Fixed side of die at ejection | Moving side of die at ejection

Figure 2 Die Surface Temperature at Ejection

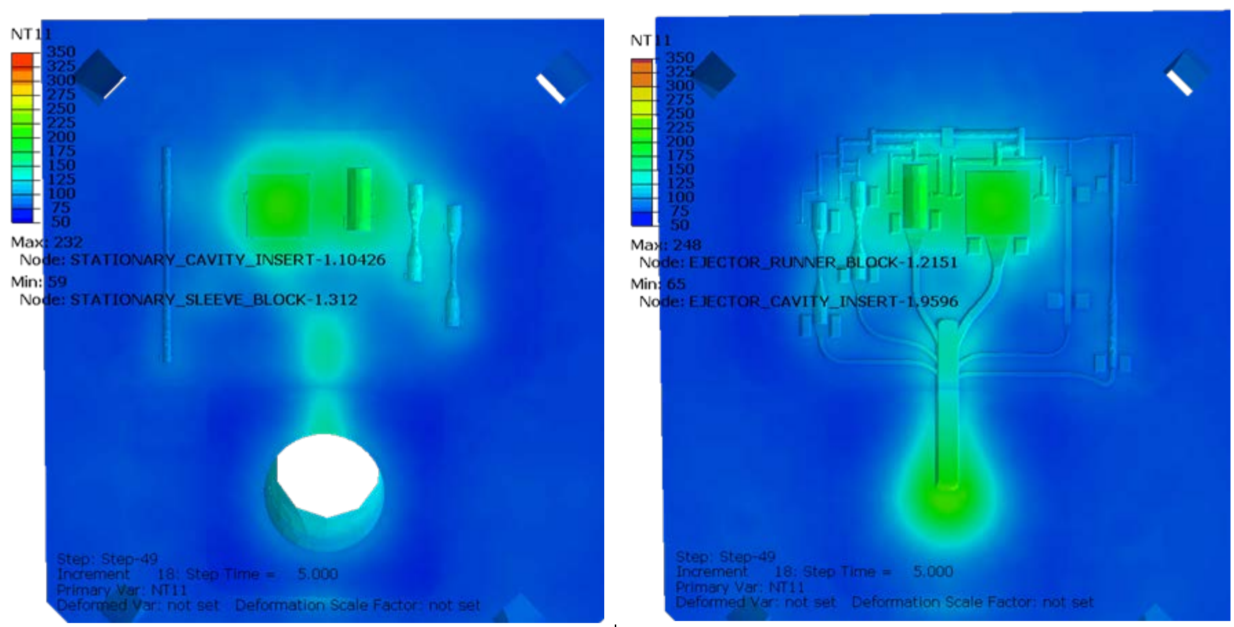

Fixed side after spray | Moving side after spray

Figure 3 Die Surface Temperature Immediately After Spray

The temperature of the entire cavity surface area, including the hot spots, is reduced about 100^oC immediately after spray. The peak temperatures are reduced but the entire distribution is also reduced by roughly the same amount and this is not necessarily a desirable result. Also, it is not shown in these illustrations, but the surface temperature recovers slightly after spray so the overall effect is less dramatic than the figures might suggest.

Spray is not a perfect mechanism for cooling, even for cooling hot spots, but it is the need to spot cool that elimination of spray will most significantly affect. Lubricant is sprayed on the entire surface when lubricant is required but it is often used for additional spray of hot spots simply because it is easier to manage – just use a little more of the same spray mixture at the location of the hot spot. If surface cooling is required for hot spots, spot spray with water, not diluted lubricant, is the preferred method and it can still be utilized in lube free casting.

These, and other factors, of die cooling are explored via the use of simple models that address the post cavity fill stage of part cooling which is the stage affected by spray. The characteristics of the basic die temperature distribution, both spatial and transient, are explored. This is followed by a sensitivity analysis that explores the relative contribution of geometric and die material properties. Different cooling strategies such as intermittent spray and no spray (let the die run hot) are considered. The conditions required for cycle-to-cycle equilibrium are then considered followed by discussion of the performance of internal cooling lines.

Model Development

The model developed for this work was a simple one-dimensional computational model with sufficient detail to develop engineering insight, but not sufficient geometric detail to use for detailed design verification. The intended use is primarily sensitivity studies and other comparative studies that illustrate the impact of various cooling strategies.

The structure of the model is shown in Figure 4. The part and die are represented by a one-dimensional slice through one side of the die. The spatial domain of both part and die are discretized and finite difference principles are used to calculate the temperature distribution within each component, one temperature value per discrete cell. The total system is then represented by a set of first order differential equations, one equation for the temperature of each cell as a function of time. A web-based application was written to read the problem setup conditions and solve for the spatial and temporal temperature history. The solution for the time response of the temperature distribution is obtained analytically after computationally finding the eigenvalues and eigenvectors of the solution. This enables additional analysis of the characteristics of the solutions, particularly the time required for the die to reach equilibrium conditions.

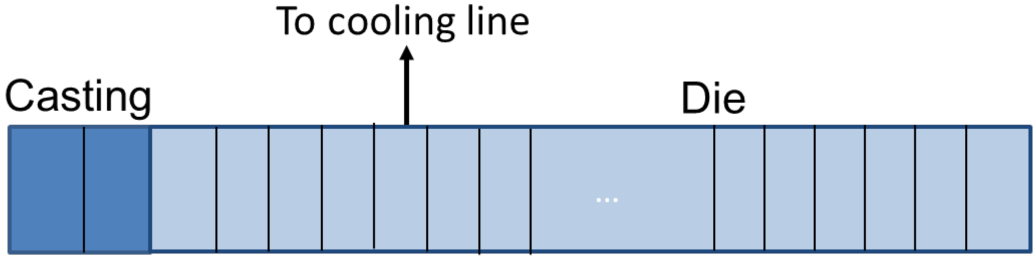

Figure 4 Depiction of Basic Model Construction

Cycle Stages and Boundary Conditions

The casting cycle as used in this work is illustrated in Figure 5. The model and boundary conditions must be adjusted at each stage to accommodate the applicable conditions.

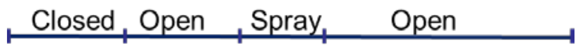

Figure 5 Cycle Segments

The overall solution is obtained by solving the system stage by stage. The model for a given stage, e.g. die closed, is configured and solved using the appropriate initial conditions. The resulting temperature distribution at the end of the stage becomes the initial condition for the next stage which is solved using the model appropriate for the stage. This process continues throughout the cycle and the process is repeated for the next and subsequent cycles. Multiple cycles are computed to examine the cycle-to-cycle variability of the temperature distribution.

The specific boundary conditions for each stage are summarized below.

Conditions common to all cycle stages:

A conduction boundary condition is placed on the insert-holder interface, i.e. the right end of the die in Figure 4. This condition models heat transfer from the die to the holder and platen of the die casting machine.

Internal cooling is approximated by a heat sink condition at the cooling line depth in the die. It is as if the cooling line is adjacent to the cell in question so that heat travels by conduction from the neighboring cells through the cell in question and is transferred to the adjacent cooling line by convection.

Die Closed

When the die is closed, the casting as well as die temperatures are modeled and heat is transferred from the casting to the die by conduction.

Die Open

When the die is open, the cavity surface of the die is exposed to air and heat transfer is modelled as natural convection to constant temperature air.

Spray

Spray is modelled as natural convection. This is accomplished by increasing the heat transfer coefficient that is used at the cavity surface. This is an imperfect model of spray cooling but it is the same approach used in most simulation modeling. It roughly accounts for the total heat removed by spray but does not account for the strong temperature dependence of the heat transfer coefficient during spray.

Results and Discussion

Basic Temperature Patterns – No Internal Cooling

The transient part and die surface temperature responses for a typical case are shown in Figure 6. A 50 s cycle is depicted with a part injection temperature at approximately 650^{o}C. The spray interval starts at 30 s, into the cycle 10 s after ejection, and lasts for 10 s. The effect of spray can be seen from the dip in the die surface temperature curve that occurs between 20 and 30 s. The temperature recovery after spray is also clear.

Note that the die temperature at the end of the cycle is the same as the starting temperature indicating that the die is in thermal equilibrium cycle to cycle.

Another important feature highlighted by Figure 6 is the fact that the die surface temperature and the part temperature are nearly the same at the time of ejection. This is a characteristic that is not always appreciated. As illustrated, the part temperature rapidly drops and the die temperature rapidly rises immediately after the cavity is filled. The rapid change in temperature is driven by the large temperature differential between the part and die. The heat lost from the part is transferred to the die causing the temperature increase, but the H13 die steel cannot rapidly diffuse the heat to the die interior. Further change in the part temperature is therefore controlled by the speed at which the die does diffuse the heat. The part and die temperatures therefore track each other during this phase of the cycle. If it were not for the fact that the biscuit (large slug of material remaining at the end of the cold chamber at the end of the shot) is generally the thickest section of the casting plus runner and is the last to solidify, the part could be ejected at or near the point where the part and die surface temperatures are nearly aligned.

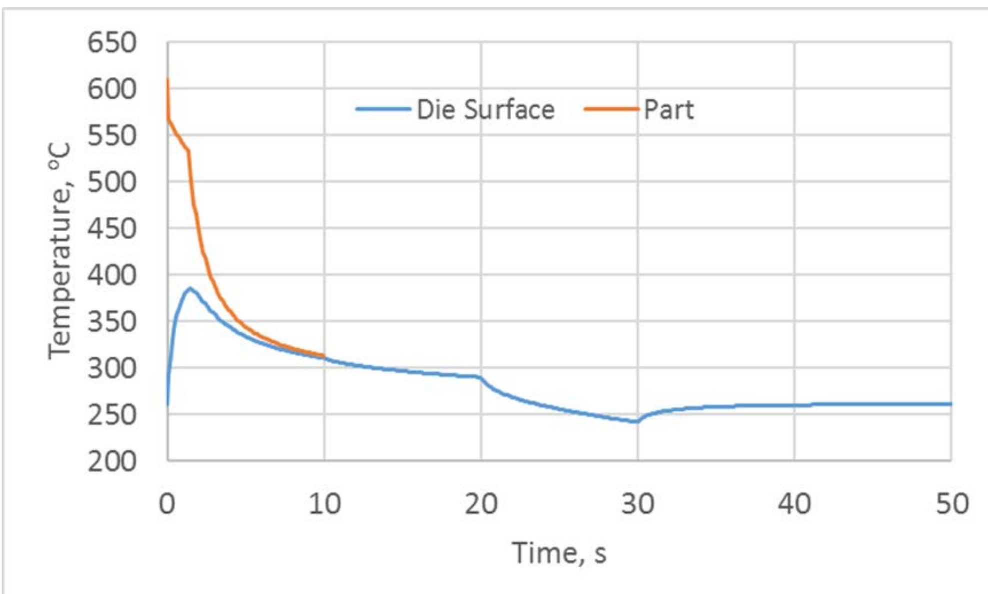

Figure 6 Baseline Transient Temperature Response

The spatial temperature distributions are shown in Figure 7. The curves illustrate the temperature distribution through the die at different stages of the cycle:

- Start and end of cycle
- At peak surface temperature
- At ejection
- Immediately before spray

- Immediately after spray

It can be seen from the figure that the rapid increase in die temperature at the start of fill does not penetrate very far into the die – about 1 cm in the figure. Most of the heat is initially held close to the surface. With additional time, heat diffuses to the interior and the surface temperature drops and by the time of ejection the heat has penetrated about 2 cm in the example. The pattern continues with the heat at the surface diffusing farther into the interior of the die and at the start of spray the penetration has reached about 3 cm. Beyond 3 cm there is very little change and the gradient is essentially constant from this point to the back surface of the die.

With the onset of spray, the surface is cooled below the surface temperature at the start of the cycle but the heat is drawn from within about 1.5 cm of the cavity surface. There is very little effect on the temperature of the interior during spray. After spray terminates, heat flows from the interior to the surface and raises the surface temperature. The fact that the temperature drops below the starting point puts the surface in a compressive-tensile cycle that is the root cause of heat checking, the primary cause of premature cracking of the die surface. Eliminating spray would help to alleviate heat checking in addition to eliminating the environmental contaminants and entrapped steam and lubricant that are sources of internal porosity in the casting.

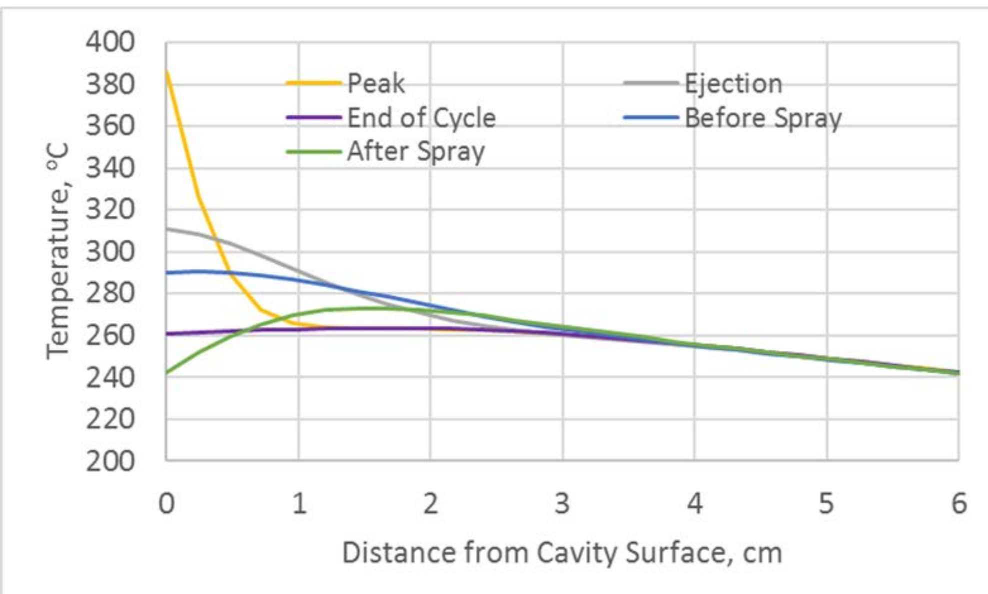

Figure 7 Spatial Temperature Patterns in the Die

The equilibrium temperature patterns must be such that the total heat extracted from the part matches the total heat dissipated by the die. The figures indirectly illustrate one of the key properties of die temperature control – the equilibrium temperature patterns establish the gradients that control the heat flow. The die temperature pattern and the part temperature are dependent variables that follow from the injection temperature, cycle timing and die properties. Die temperature and part injection temperature are not independent variables that can be arbitrarily set ahead of time as is sometimes assumed.

Effects of Internal Cooling

The use of internal cooling is the primary tool available to control die temperature. The presence of a cooling line will modify the spatial temperature profile as illustrated in Figure 8. In this case the cooling line is placed about 2.5 cm or 1 inch below the surface. The temperature profile is essentially static below the cooling line and the dynamic response is between the line and the surface. The spray effect is similar to that shown in Figure 7 causing the temperature to drop below the temperature at the cycle start and then recovering by drawing heat from the interior of the die.

Figure 9 illustrates the same case without spray. Note that the die surface temperature is slightly higher at each stage of the cycle without spray, but the spatial patterns are essentially the same. Elimination of spray with no change in internal cooling therefore results in a hotter running die due to less total heat removal. The most important observation is that the spray effect on the temperature in the region close to the surface is short-lived and does not significantly impact the temperature pattern. The bigger effect of spray is on the overall die bulk temperature since the spray removes heat from the surface and this heat therefore does not have to diffuse to the interior of the die.

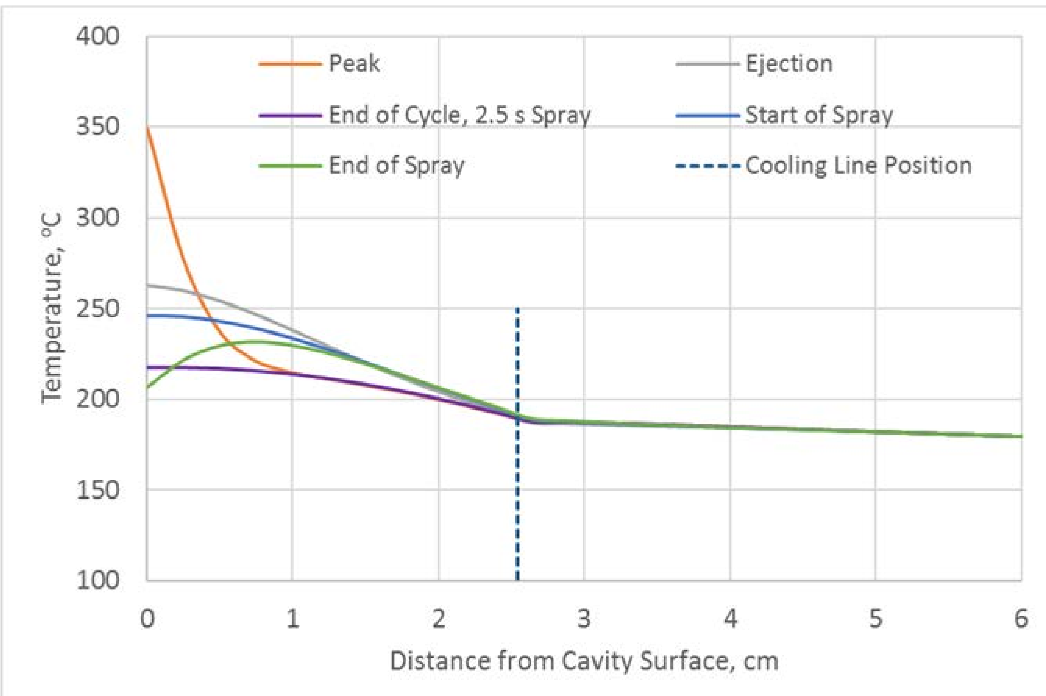

Figure 8 Effect of Cooling Line on Spatial Temperature Distribution

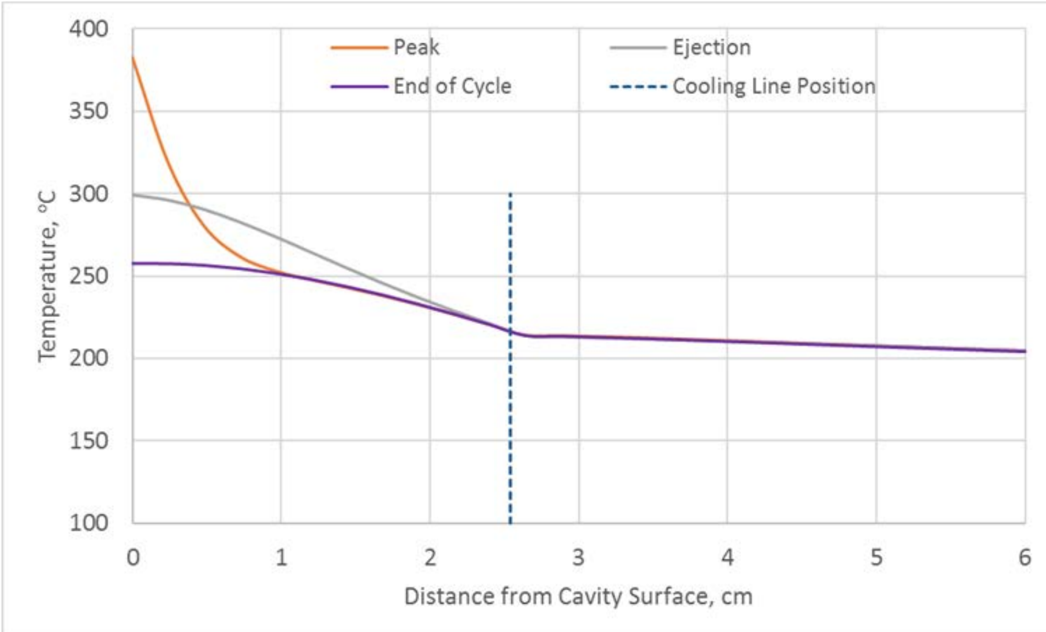

Figure 9 Cooling Line Without Spray

Another illustration of the effect of spray is illustrated in Figure 10 which plots die temperature at the start of the cycle as a function of spray interval. The longer the spray interval, the more heat removed as shown in the figure. The effect of increasing the spray interval is to lower the entire temperature curve.

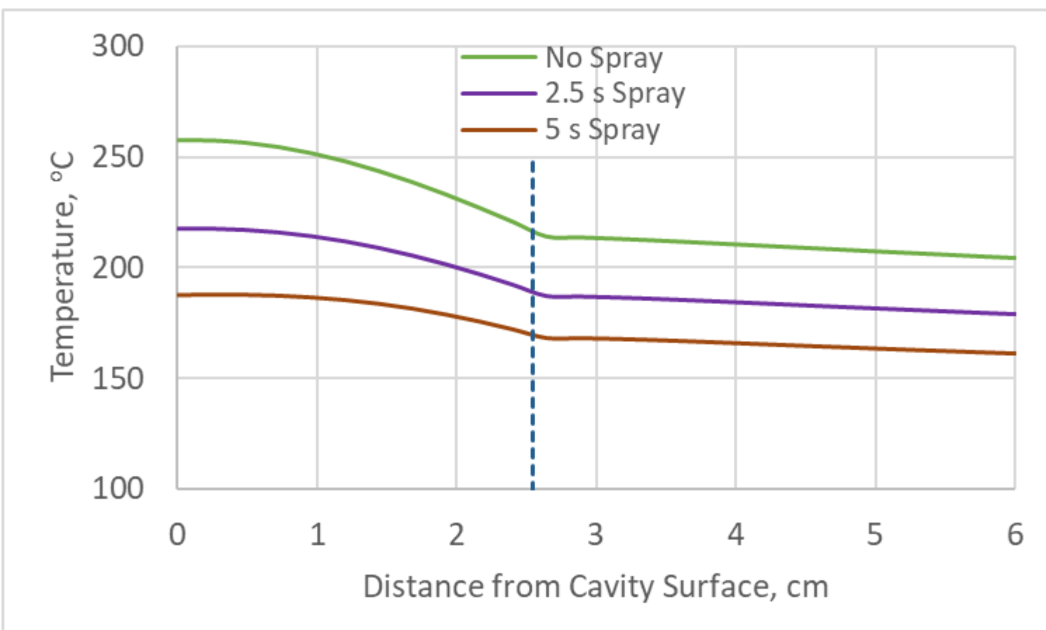

Figure 10 Comparison of Spray Interval Effects

Figure 11 shows the effect of cooling line depth on the die temperature at the start of the cycle. No spray cooling is included in this comparison. The deeper the line, the higher the average die temperature and the die surface temperature.

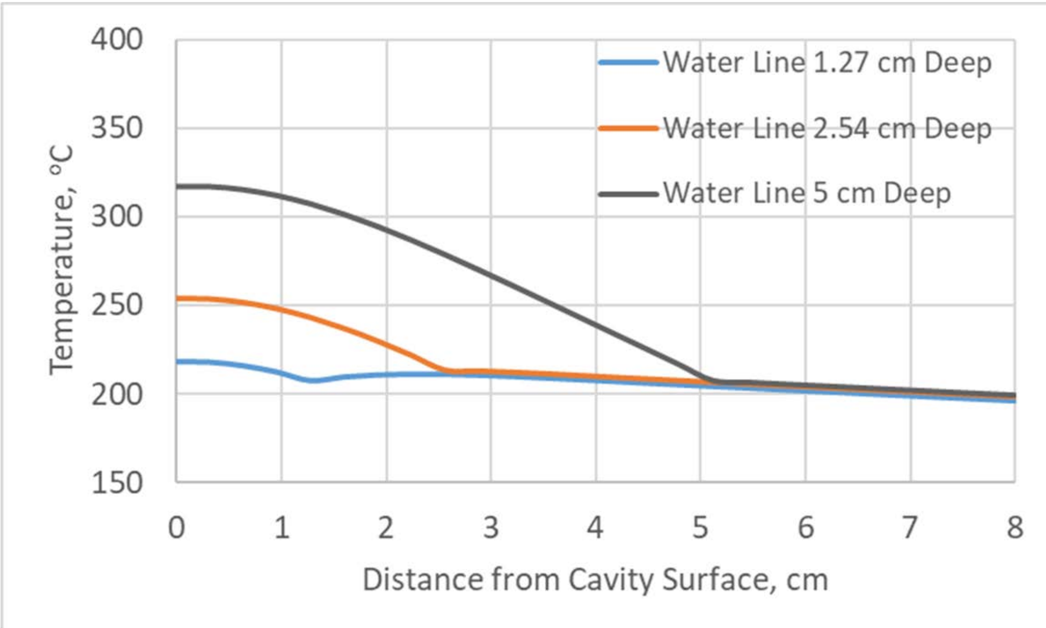

Figure 11 Comparison of Cooling Line Depth Effect, No Spray

In summary, both spray and cooling line placement affect overall die cooling. The longer the spray, the lower the average temperature; the closer the cooling line is to the surface, the lower the average temperature.

We now turn to examining some of the strategies suggested to accommodate the elimination of spray.

Let the Die Run Hotter

One approach to cooling in the absence of spray that is sometimes suggested is to make no adjustments and simply let the die run hotter. While this might work in some instances, it may result in unstable operation. To illustrate, consider the differences between Figure 12 and Figure 13. Figure 12 is the baseline and the die temperatures at each stage are quite reasonable.

Without spray, as shown in Figure 13, by cycle 25 the temperature near the surface is roughly 100^{o}C hotter and the gradient is noticeably steeper to support more heat flow to the rear surface of the die. The biggest problem, however, is that the die is still far from equilibrium. Because no heat is removed by spray, the overall die temperature must rise, reducing the heat extracted from the part and increasing the heat dissipated through the back surface of the die and to air when the die is open. Figure 14 shows that it takes at least 100 cycles to reach quasi-equilibrium in this case and the die runs about 200^{o}C hotter than with spray. This may be too hot resulting in part ejection before sufficient casting strength is achieved.

Note that internal cooling was not increased in this example and the total effect is not necessarily representative of any specific case, but it does illustrate that the strategy of doing nothing to accommodate the elimination of spray may not be feasible.

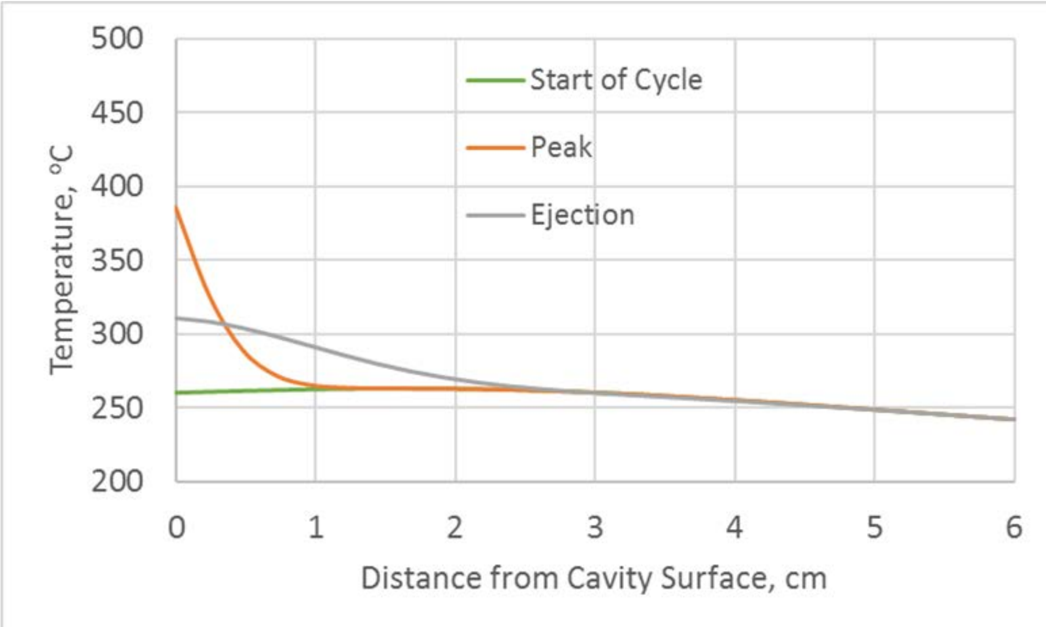

Figure 12 Spatial Distribution with Spray, Cycle 200

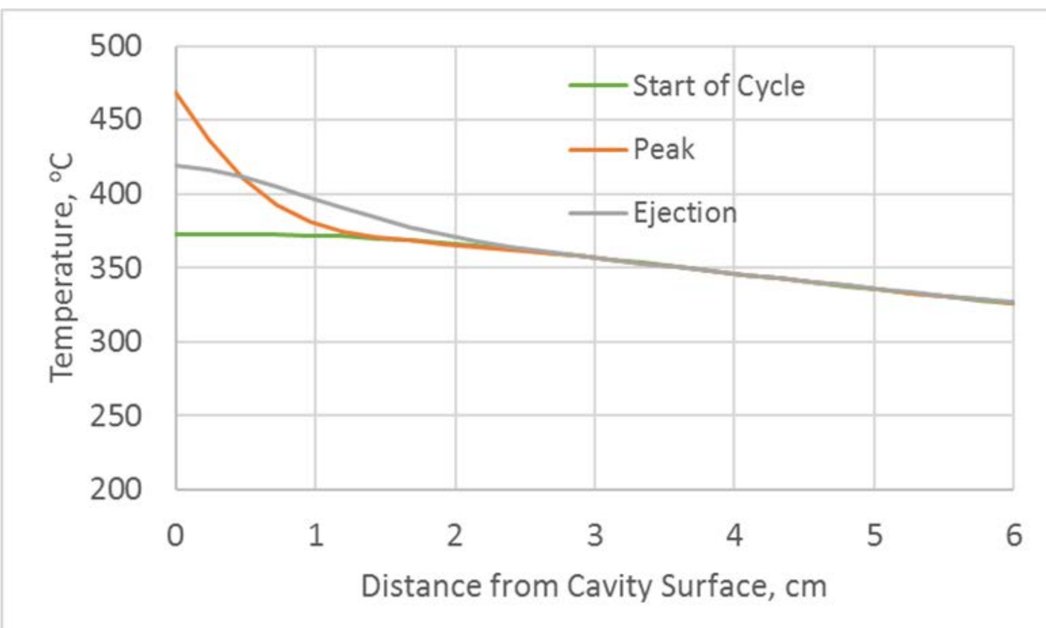

Figure 13 Spatial Distribution, No Spray, Cycle 25

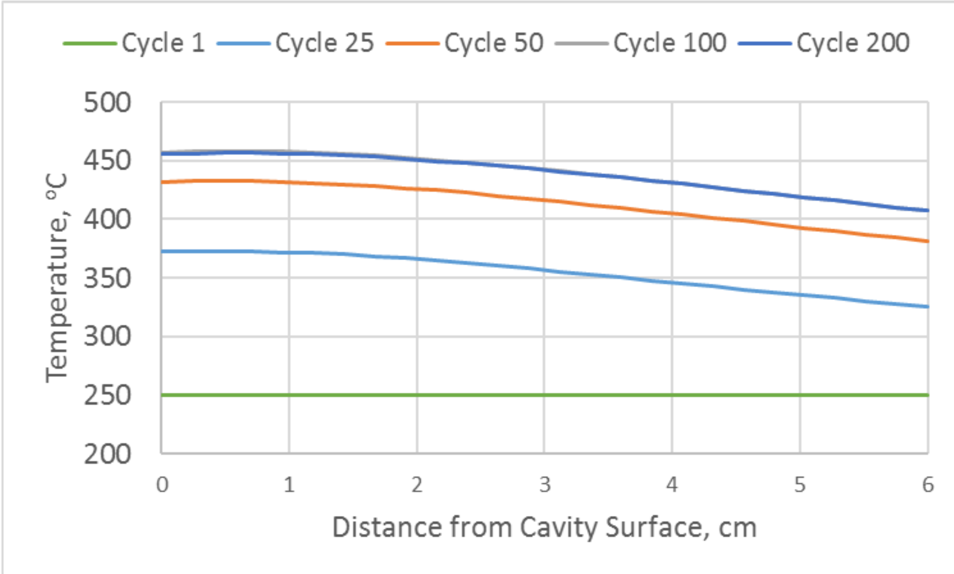

Figure 14 Cycles to Quasi-Equilibrium

Figure 15 and Figure 16 provide the transient responses corresponding to the spatial plots presented in Figure 12Figure 13. The higher temperature without spray is clear. The peak temperature is delayed due to the smaller temperature differential between the part and die in the absence of spray, but the overall transient pattern is basically the same.

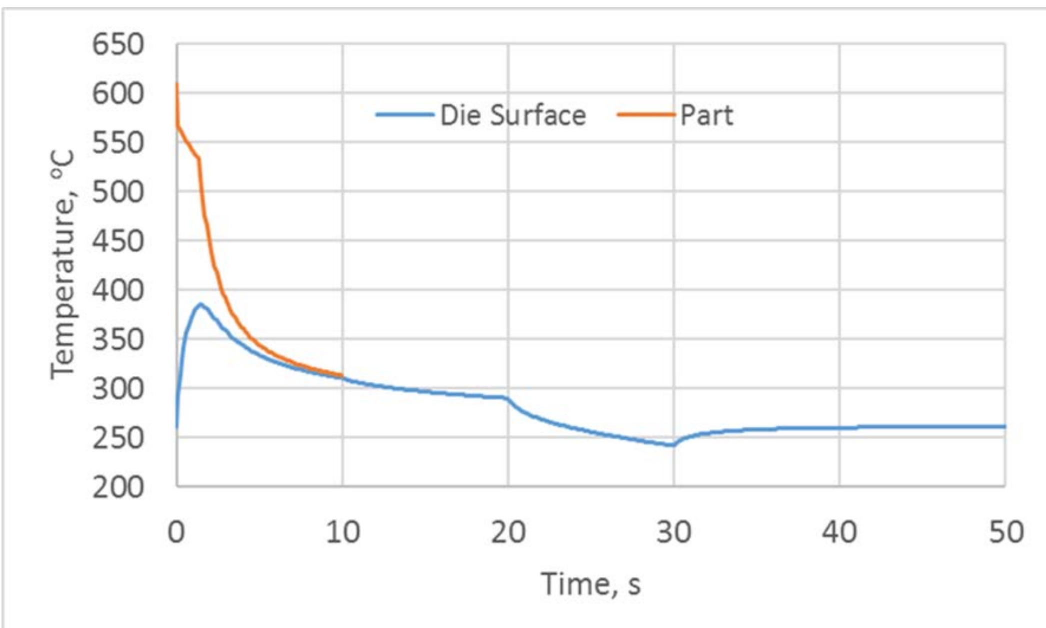

Figure 15 Transient Response with Spray, Cycle 200

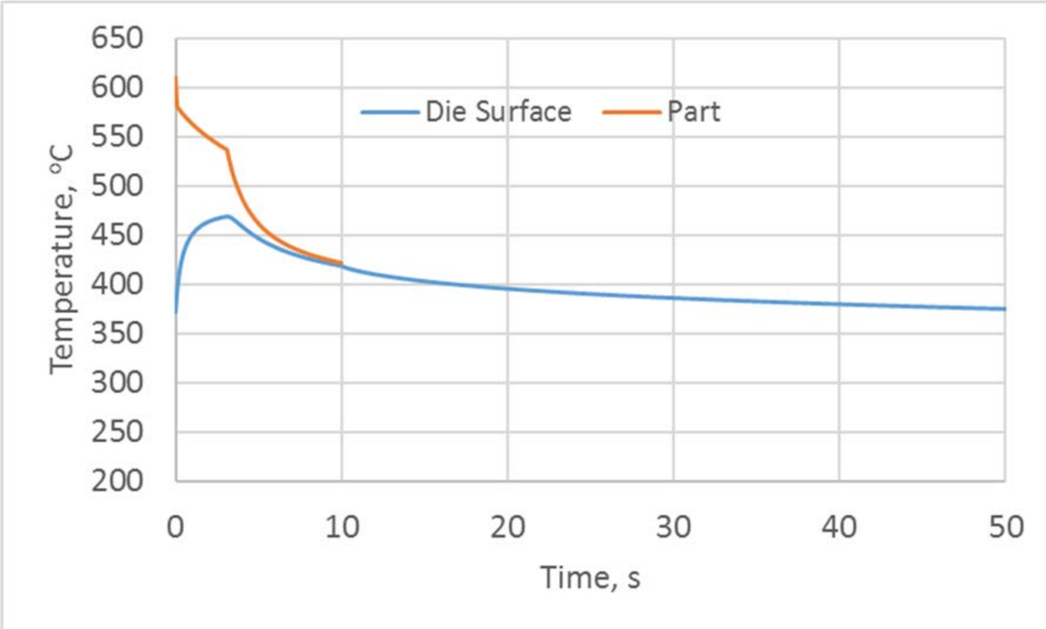

Figure 16 Transient Response without Spray, Cycle 25

Intermittent Spray

Another suggestion to reduce spray utilization is spray intermittently, for example every 10th cycle instead of every cycle. This would reduce total spray utilization and yet might provide sufficient cooling. An example of this strategy where spray is applied every 10th cycle is shown in Figure 17. The transient responses for the spray cycle along with the cycles before and after spray are shown. As can be seen, the temperature is reduced by spray and then gradually increases until the next spray cycle, creating a pattern of slowly varying die temperatures that rise and fall around the spray cycle. This strategy could be effective but the die temperature would never achieve quasi-equilibrium and the part ejection temperature band would be larger than would be obtained with a cooling approach that is consistent across cycles. This added variability could be significant when trying to hold tight dimensional tolerances that requires precise temperature control.

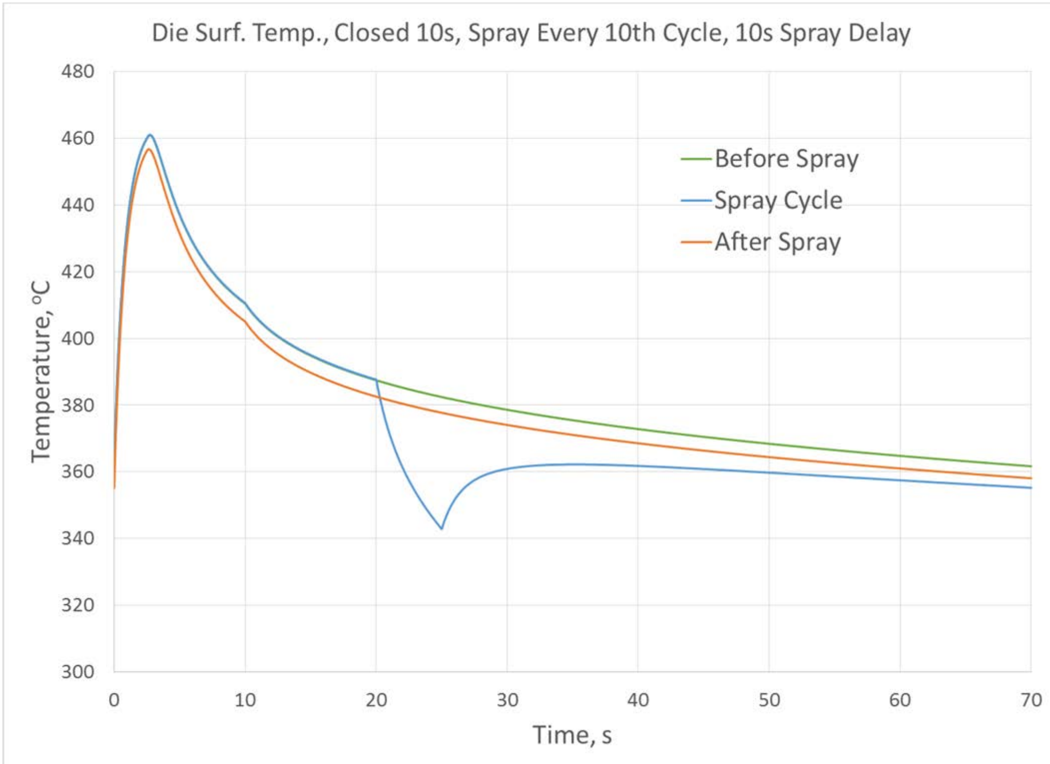

Figure 17 Effect of Spray Every 10th Cycle

Increase Cycle Time

Another approach to accommodate for elimination of spray is to increase the total die open time allowing conduction and natural convection to cool the die. Figure 18 is an illustration of this approach. In this specific case, increasing the cycle from 45 s to 70 s provides sufficient time for the other cooling mechanisms to compensate for lack of spray. Note that the part temperature curves are nearly indistinguishable and the die surface temperatures are also essentially the same at the start of the cycle. The cooling is therefore effective, but at a significant penalty in cycle time and therefore a significant productivity penalty.

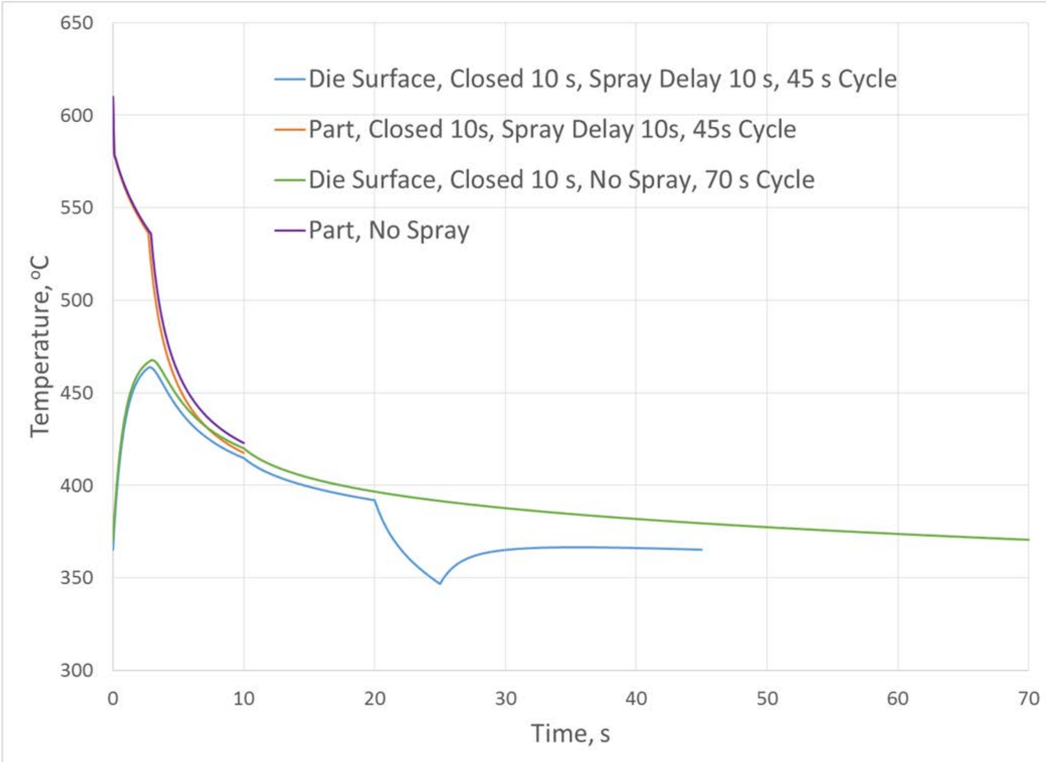

Figure 18 Increasing Cycle Time to Account for Elimination of Spray

A Sensitivity Study

While not directly related to the die cooling issue, the question of how the die material affects the temperature distribution and the cooling response is of importance for understanding what factors control the die temperature response. The thermal response of the die depends primarily on the density, thermal conductivity, and specific heat of the material. The heat transfer coefficient at the part-die interface is the other factor of importance. Table 1 includes a comparison of the key material properties of H13 tool steel, copper and tungsten. This is not to suggest that the materials are suitable die materials but only to compare thermal performance.

Table 1 Comparison of Properties

	Tungsten	H13	Copper
Density, ρ (g/cc)	19.3	7.8	8
Specific Heat, c_p (J/g °K)	0.134	0.46	0.385
Thermal Conductivity, k (W/cm °K)	1.63	0.24	3.85
Volumetric Spec. Heat, ρc_p (J/cc °K)	2.59	3.59	3.08

H13 and copper have comparable densities and specific heats but differ by more than an order of magnitude in thermal conductivity. Also, tungsten has higher conductivity, but because of the large density, the diffusivity is close to that of H13. The diffusivity of copper is an order of magnitude higher. The range of these parameters allows for an examination of the potential benefits of a very higher conductivity and higher diffusivity die materials.

A four factor, three level per factor, computational experiment was completed to explore the effects of the die material. The factors and levels are shown in Table 2. The levels for the heat transfer coefficient correspond to the typical range used in simulation models for part cooling. The levels for the material properties are taken from Table 1. The response variable was the die surface temperature at the start of the cycle.

Table 2 Factor and Level Definitions

	Low	**Mid**	**High**
HTC ($W/m^2\ {}^oK$)	3000	5000	7000
Die Depth (cm)	6	9	12
Thermal Conductivity, k ($W/cm\ {}^oK$)	0.24	1.63	3.85
Volumetric Spec. Heat $\rho\ c_p$ ($J/cc\ {}^oK$)	2.59	3.08	3.59

The interaction plots of the results are shown in Figure 19. The main effects are shown in Figure 20. Considering the interactions first, the most interesting result is the saturation of conductivity. An increase in conductivity from the low level (H13) to the middle level results in a lower die surface temperature, but a further increase in thermal conductivity has essentially no effect. This is true at all heat transfer coefficient levels, all volumetric specific heats, and all die depths. As will be shown shortly, this is because at very high conductivity, temperature changes propagate rapidly through the die and the die temperature level is controlled by the capacity of the heat sinks to extract heat. In other words, with very high conductivity it is convection to the surroundings and to the cooling lines that will ultimately control temperature. High conductivity will only help if the heat sinks have sufficient capacity.

It is also interesting that die depth has no effect. This can be seen by the fact that all curves in the bottom row of the plot are essentially coincident.

Increasing the heat transfer coefficient results in a lower die surface temperature. This is true for the levels tested, but if the heat transfer coefficient is extremely low, the trend is in the opposite direction but under such conditions the die temperature is such that part ejection temperatures are excessive for reasonable cycle times.

The same tendencies are apparent in the main effects shown in Figure 20. There is a significant drop in temperature from the lower conductivity H13 to the intermediate level.

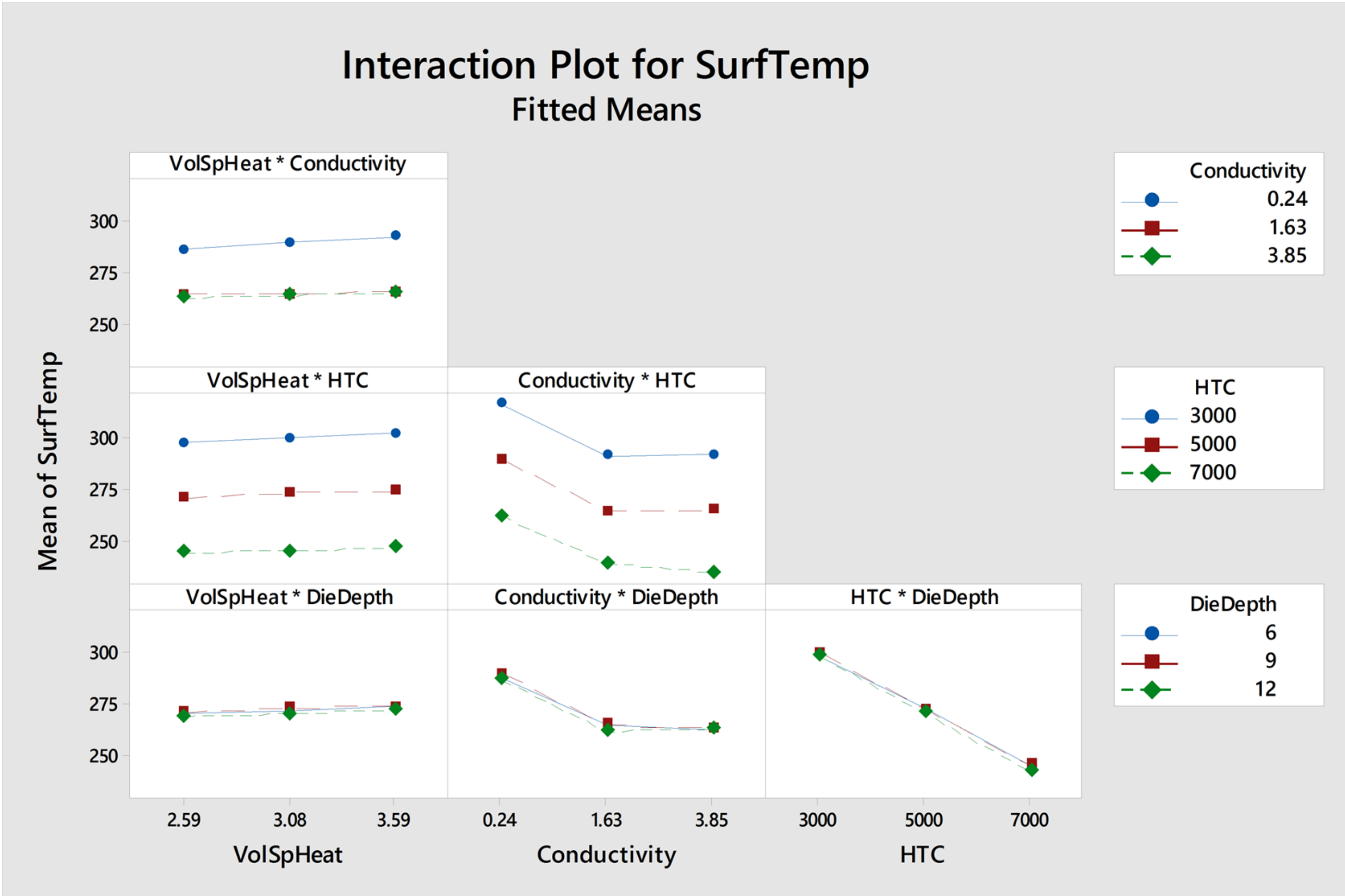

Figure 19 Interaction Plots

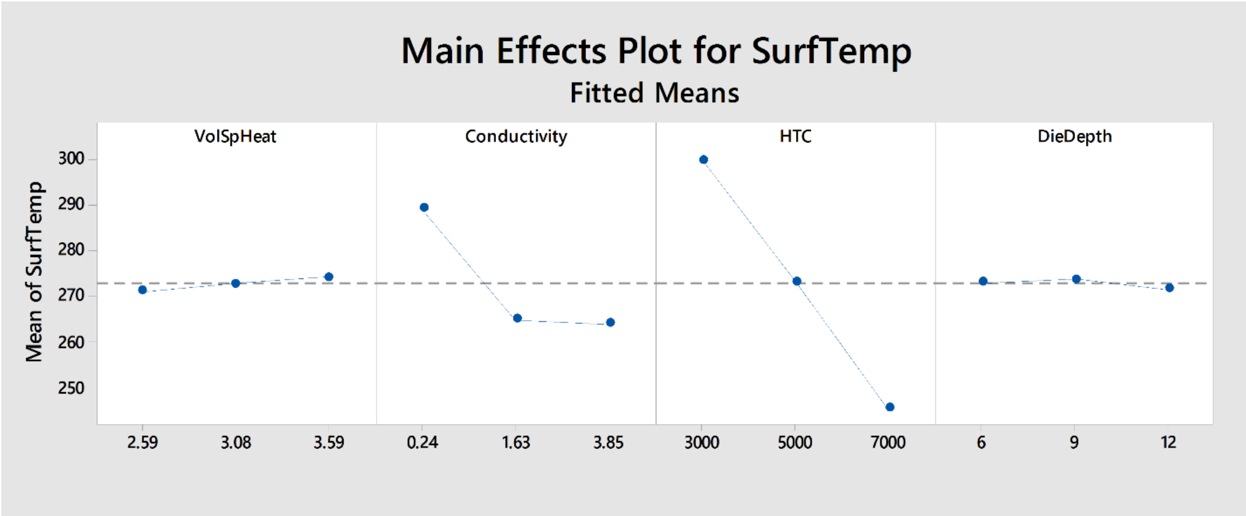

Figure 20 Main Effects Plots

The benefits of a higher conductivity material are perhaps easier to understand with a comparison of the transient and spatial responses. The following examples are constructed using the same process conditions and a cooling line at 2.5 cm from the die surface. As can be seen from Figure 21, the peak temperature is much lower with the higher conductivity material and there is less overall temperature variation. The part ejection temperature is similarly lower. There is less difference in the die surface temperature at the start of the cycle. Clearly the higher conductivity material extracts heat and dissipates it through the die more quickly.

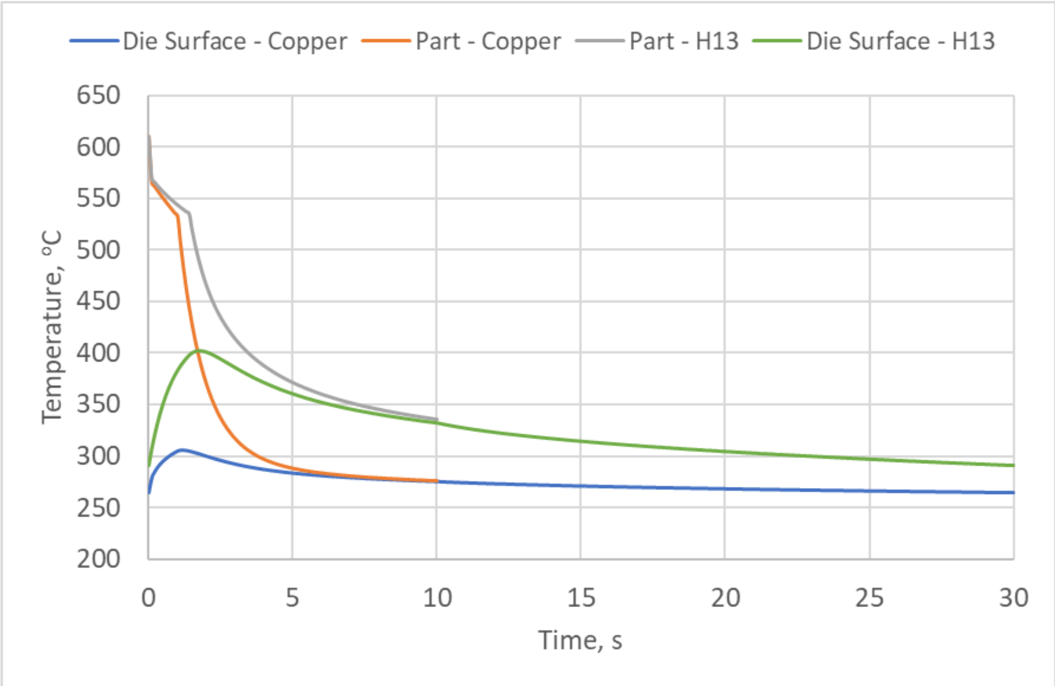

Figure 21 Transient Response Comparison – Effect of Conductivity

The spatial responses for the two materials are shown in the next two figures. The effect of the cooling line is much more obvious in the H13 case. The distance over which the temperature dynamically changes is nearly the full depth of the die in the high conductivity case and the gradient runs slightly from the back surface to the cooling line for part of the cycle. The limits imposed by cooling are due to this pattern.

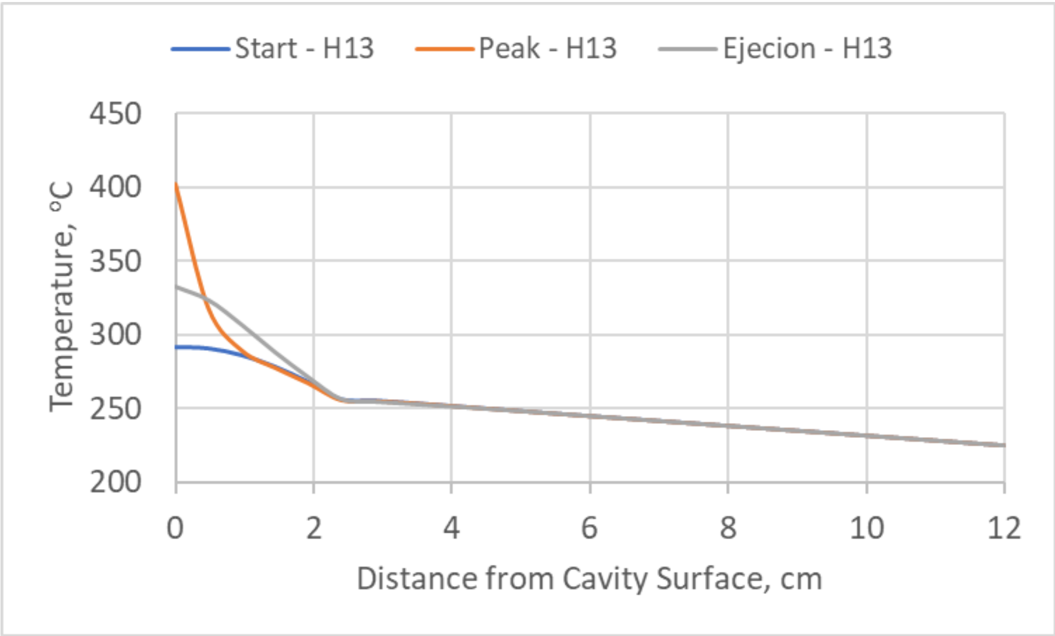

Figure 22 Spatial Distribution, H13

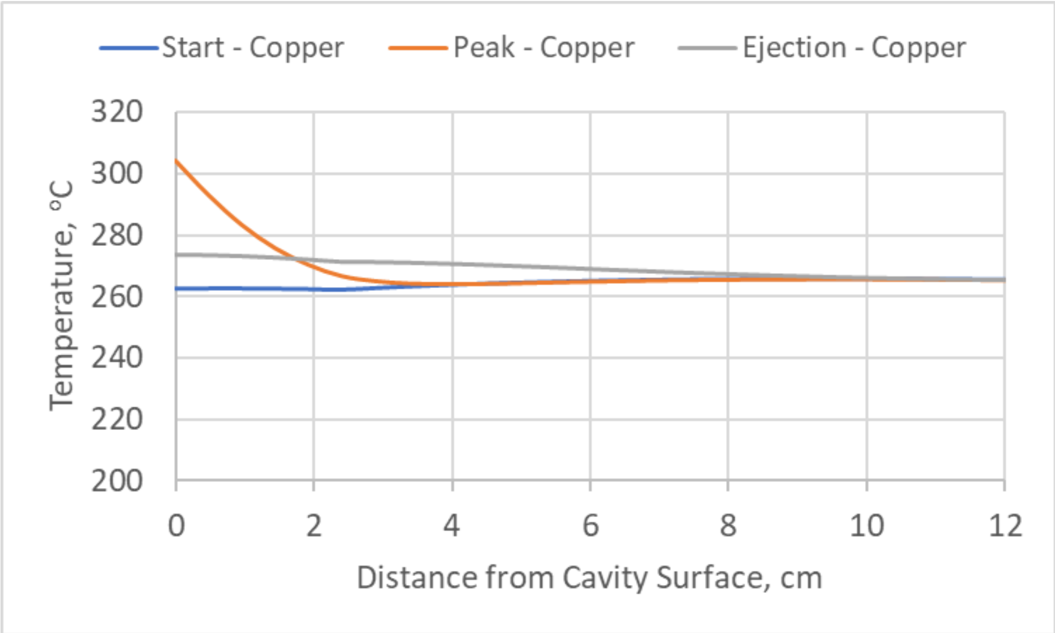

Figure 23 Spatial Distribution, Copper

In summary, higher conductivity materials would enable more rapid removal of heat and would reduce the range of temperature oscillations in the die, but such improvements also require the capacity to dispose of the heat to the environment. The heat sinks become the bottleneck.

The fact that the die thickness has no or little effect on die surface temperature may also be surprising to some. The size of the die determines the total thermal mass which controls how rapidly the die responds to change including how rapidly it will warm up of cool down. This can be seen from the eigenvalues of the model as reported in Table 3. The smallest eigenvalue or time constant in each case determines how long it takes for the system to achieve equilibrium. The largest eigenvalue determines how quickly the die responds at the onset of a perturbation, e.g. how quickly the temperature starts to change after completion of fill. It is clear from the table that both the largest and smallest magnitude eigenvalues increase with decreasing thickness (i.e. thinner dies respond more quickly and reach equilibrium more quickly.) Comparing the high and low conductivity materials, the difference in the largest magnitude eigenvalue is much greater than the smallest. This means that the high conductivity material will start to respond quickly and will form the basic spatial distribution quickly, but the die will not reach equilibrium significantly faster than the lower conductivity material. In other words, the high conductivity material will not warm up significantly faster than the lower conductivity material. More information about time constants and the relationship to equilibrium can be found in (Miller 2016).

Table 3 Cycles to Equilibrium

	Smallest Magnitude Eigenvalue (/s)	Largest Magnitude Eigenvalue (/s)	Rough Estimate of Max Cycles to Convergence
H13, 12cm	-0.0008	-1.02	190
H13, 6cm	-0.0018	-4.11	85
Copper, 12cm	-0.0011	-19.3	140
Copper, 6cm	-0.0023	-777.0	70

Cooling Line Design and Performance Characteristics

The development of the mathematical relationships used in this section is included in the Appendix. The development includes a brief summary of how the total heat transfer rate is determined, how to compute the appropriate heat transfer coefficient, and derivation of the basic design equations.

The heat transfer coefficient for a cooling line can be computed using Equation (7) in the Appendix. Illustrations of the heat transfer coefficient as a function of linear speed and flow rate for several line diameters, assuming water is the coolant, are shown in Figure 24 and Figure 25. The jump due to the onset of turbulent flow is clear, particularly in Figure 24.

The difference between the two figures is visually striking and most easily explained by noting that the flow rate is the speed multiplied by the cross-sectional area of the line which is proportional to the square of the diameter. Note that all curves in both figures terminate at approximately the same heat transfer coefficient magnitude and in Figure 24 the speeds at which the maximum is reached for the four cases are relatively close to 2 m/s. The square of the diameters however varies by a factor of nearly 5, i.e., from 36 to 169 mm^2. This multiplier explains the separation of the curves when plotted against flow rate.

Figure 26 provides the same information as Figure 25 but with the flowrate scale restricted to 10 L/min, a little more than 2 gal/min. Clearly, the fact that the smaller the diameter of the line, the larger the heat transfer coefficient at a given flowrate. It is difficult to provide a simple explanation for the phenomena since the Nusselt number, Reynolds number and heat transfer coefficient are all interrelated and dependent on both flowrate and diameter. The figure itself is perhaps the best explanation.

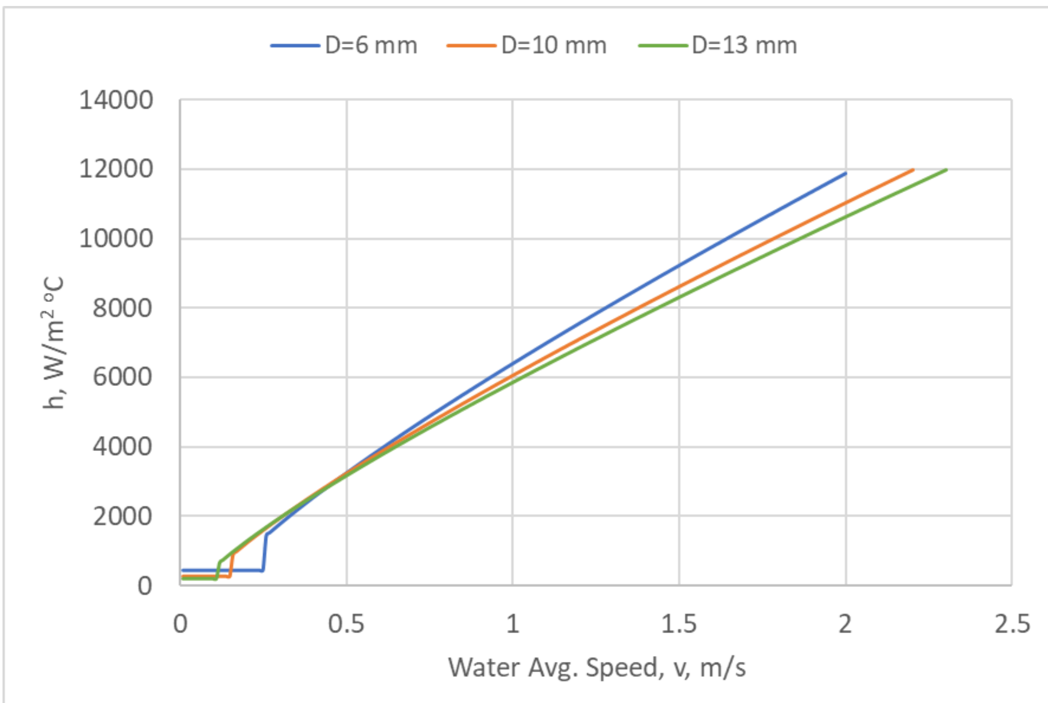

Figure 24 Heat Transfer Coefficient as Function of Linear Speed, Water Coolant

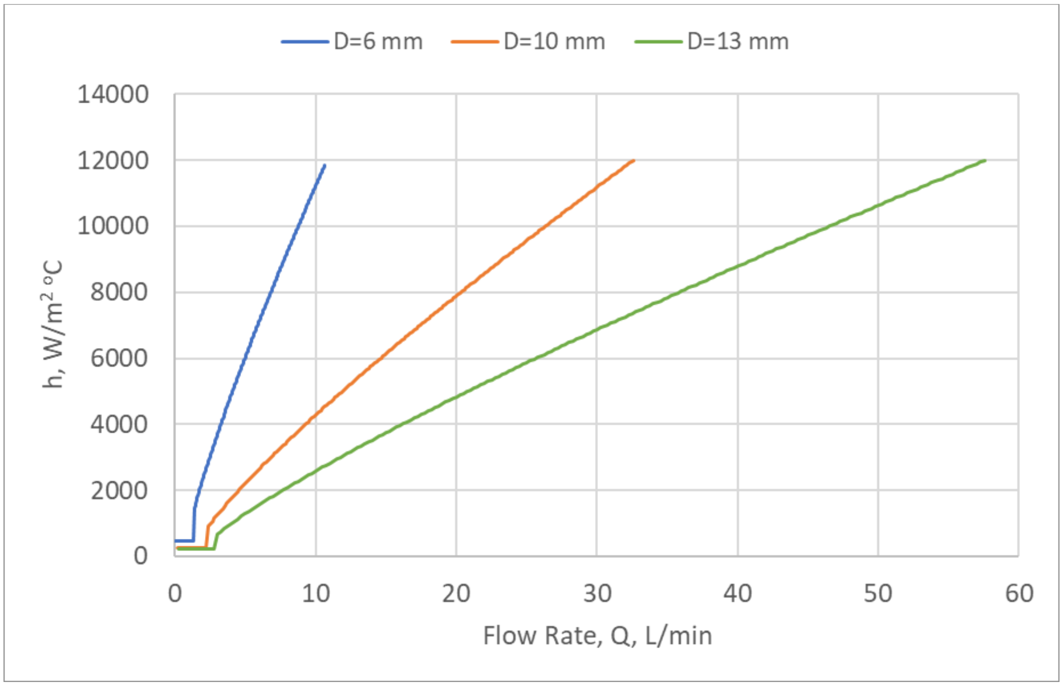

Figure 25 Heat Transfer Coefficient as a Function of Flowrate, Water Coolant

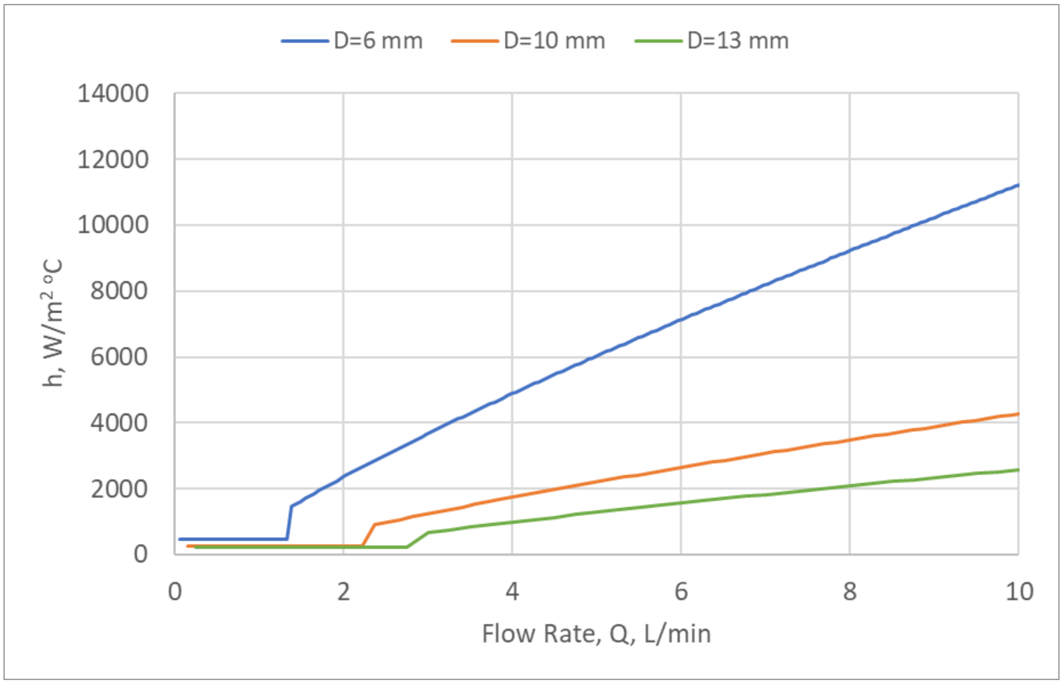

Figure 26 Heat Transfer Coefficient as a Function of Flowrate, Expanded Scale

The heat transfer coefficient is only part of the cooling line performance story. Equation (12) in the Appendix captures the change in coolant temperature as a function of distance. A comparison of temperature difference versus distance as a function of line diameter and flow rate is shown in Figure 27. The water inlet temperature and die temperature used are 40ºC and 175ºC respectively. The results are very sensitive to the coolant and die temperature values.

Since the inlet temperature is 40ºC, the maximum change that can occur without boiling is 60ºC. All curves in the figure are terminated at approximately 60ºC. The increase in distance with increasing diameter for a given temperature difference is due to the additional mass in larger lines. The curves show that the temperature change is more sensitive to the line diameter than to the flowrate. The temperature change increases at smaller diameters. The relative position of the curves change as the diameter is increased due primarily to the heat transfer coefficient behavior. The temperature differential is larger for lower flowrates at small diameters, but reverses and is larger for higher flowrates at larger diameters but the differences are small. The temperature differential is relatively insensitive to flowrate.

The total heat removal rates are shown in Figure 28. This result is intuitive in that heat removal rate increases with flow rate for lines of the same diameter. Note however, for any fixed length, the total heat removal rate increases with flow rate and decreases with diameter. For example, a 6 mm diameter, 0.4 m long line running at 4 L/min removes more heat than a 10 mm diameter line of the same length and running at the same flowrate. As can be seen from either Figure 27 or Figure 28, the smaller lines reach the maximum ΔT at a shorter distance, but the smaller lines have a higher total heat removal rate at lengths for which they are feasible.

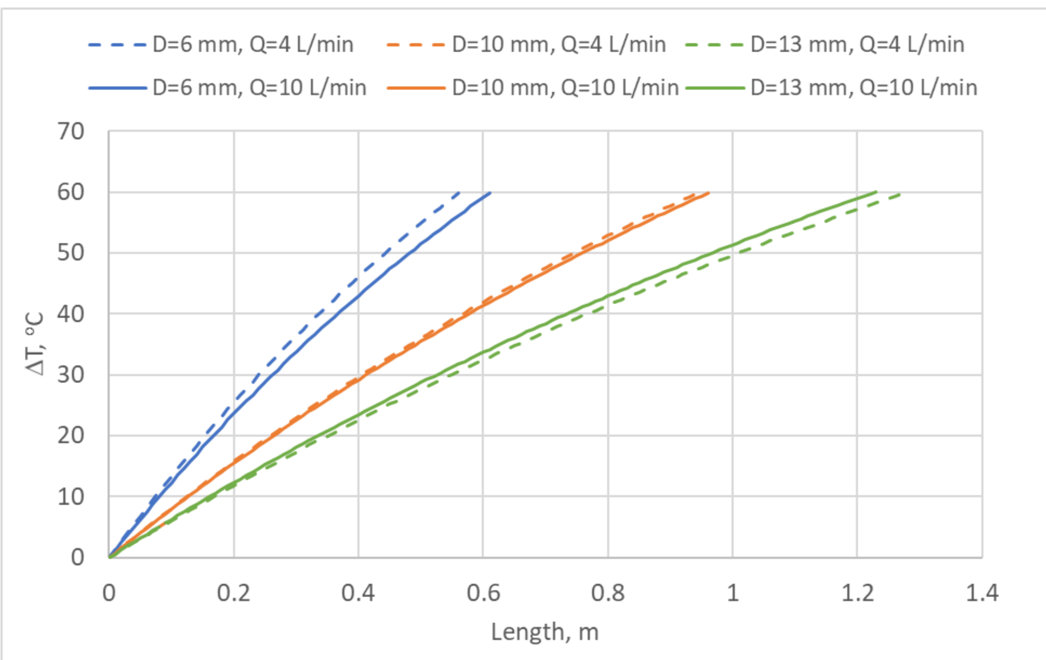

Figure 27 Water Temperature Rise as a Function of Distance

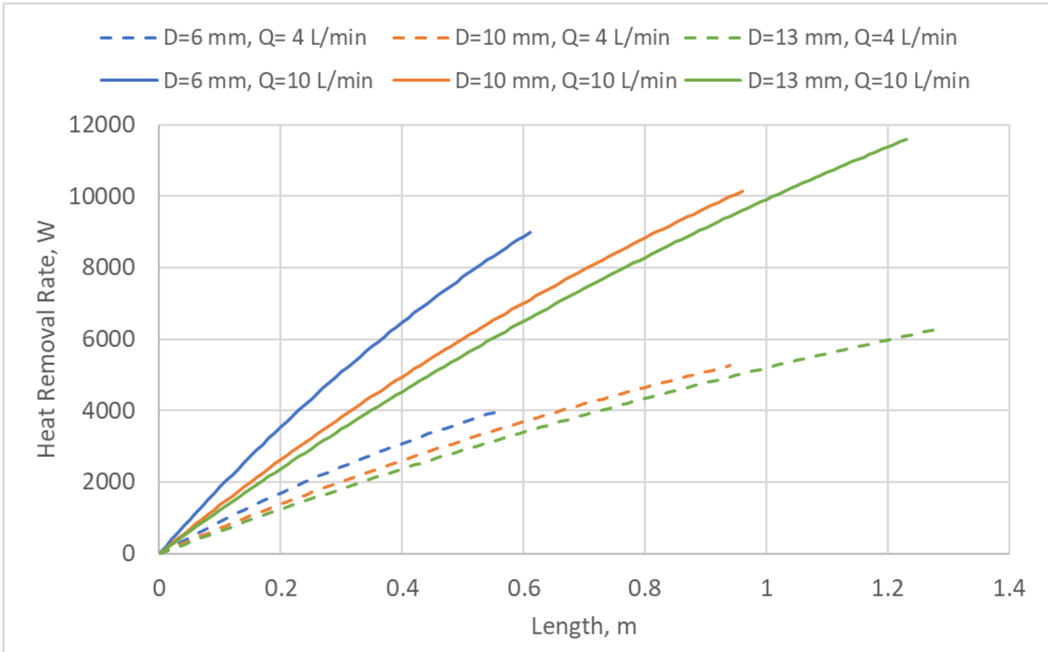

Figure 28 Total Heat Removal Rate as a Function of Distance

Outline of Design Procedures

There is no single procedure to design a cooling line or to determine the cooling load that must be accommodated. The actual procedures will depend on company practice and standards and the detailed geometry of the die cavity. However, the key relationships and variables can be summarized.

The main relationships needed for cooling line design are:

- Equation (7), the heat transfer coefficient, which depends on the Nusselt number correlation, Equation (4).
- Equation (12) in the appendix which defines the temperature increase in the cooling medium,
- Equation (16) in the appendix that relates the total heat transfer rate to the design variables.

The input variables required of the designer are:

- Coolant inlet temperature
- Die surface temperature
- Required heat transfer rate &

The design variables are:

- Line length L
- Line diameter D

- Flowrate Θ
- Acceptable temperature rise, $\Delta T = T_{outlet} - T_{inlet}$

The exact solution procedure depends on which variables are fixed by standard practice or preference. For example, the length of the cooling line, L, is often constrained by the size of the insert. The designer or caster may have preferred line diameters and flowrates in which case temperature rise is the only free variable and it can be computed using Equation (16). If the result is not acceptable, one or more of the inputs must be adjusted.

If the temperature rise is specified, Equation (12) can be used to find the line length or diameter. This also requires that the flow rate be computed using Equation (16).

In general, iterations are required until all conditions are met and all design variables have acceptable values.

Comments About the Field Test Die

The field tests of the coated die performed at Mercury Marine Castings demonstrated that casting with minimal spray is feasible and seems to enable a shorter, more consistent cycle. Additional internal cooling was designed into this die and worked effectively. The results of the previous section that characterize cooling line performance explain why.

To illustrate, consider the data in Table 4 that summarizes estimates of the key thermal characteristics of the part and process. The part mass and material properties are accurate but the actual process and die design data are proprietary so estimates are used for the illustration.

Based on the estimates, and comparing against Figure 28, 6 mm lines running at 4 L/min would provide adequate cooling to dissipate all heat assuming two lines and equal heat loads in each half of the die. The die temperature near the lines is assumed to be approximately 175^{o}C. Six, 10 or 13 mm diameter lines would all work at flowrates near 4 L/min. In other words, any pair of lines operating at a low flowrate would provide sufficient cooling even with water at a relatively high 40^{o}C inlet temperature. A lower inlet temperature would provide even more cooling. Figure 27 shows that the temperature rise in the coolant would be between 10^{o}C and 25^{o}C depending on the line diameter.

For comparison, if a single line were used on each side of the die, the heat rate would be about 3100 W per line and the 6 mm lines would still be feasible but a flow rate near 10 L/min would be needed. Larger diameter lines would require a flowrate exceeding 10 L/min.

In summary, it is not surprising that the field tests were successful (from a cooling perspective). The conservative estimates used in the above analysis clearly show that the die can be adequately cooled with internal lines.

Table 4 Approximate (Estimated) Conditions for Field Test Die.

Quantity	Estimated Value
Part Mass	795 g
Part Injection Temperature	620 ^{o}C
Part Ejection Temperature	300 ^{o}C
Latent Heat	388.44 J/g
Specific Heat	0.963 J/g ^{o}K
Cycle Time	40 s
Total Heat Load	245,000 J each cycle
Heat Rate = Total Heat Load/Cycle Time	6125 W
Line Length	0.2 m
Number of Cooling Lines in Cavity Area	4 (2 each side)
Heat Rate per Line	1531 W
Estimated Line Requirements	6 mm diameter, 4 L/min flowrate

Conclusions

The elimination of lubricant spray eliminates a widely used cooling mechanism. It is estimated that as much as 30% of the die cooling is accomplished via spray in many instances. But, this is a chicken and egg situation. Spray is needed for lube and provides cooling; therefore, internal cooling is reduced. It is not the case that internal cooling is incapable of meeting the die cooling requirements. This has been demonstrated in the past by select casters who have designed dies to run with a minimal amount of spray. The results of this work confirm that elimination of spray presents no significant problem to die cooling system design. However, cooling system design and the thermal response of dies is imperfectly understood by many die casters and many of the results of this research can be used to improve the materials used to teach cooling system design principles.

It must be noted that spot cooling of hot spots may be an issue in some geometries and spray may still be required for this purpose but the spray does not have to include lubricant. Spray of water, not diluted lubricant, is the preferred method to spray cool hot spots. Newer technologies such as jet cooling, internal spot cooling, and conformal cooling all provide internal methods for addressing the problem. The key point is that lube free die casting does not have to mean complete elimination of spray cooling if the part geometry demands local external cooling.

Summary of Results

This work has demonstrated several of the key physical principles that underlie die thermal response and cooling design. A simple one-dimensional model was used to perform several sensitivity studies that illustrate the tradeoffs inherent when spray cooling is reduced or eliminated.

It is commonly stated that spraying the die affects the temperature close to the surface and this is true particularly in the short term. But, the modelling shows that the bigger effect is a long-term increase in the bulk temperature of the die. Spray rapidly cools the die surface and when spray stops heat flows from the die interior to the surface resulting in a lower overall temperature.

It was shown that "letting the die run hot" by eliminating spray, but making no adjustments to the cycle or to internal cooling, may work in some instances but it may also result in thermal instability. The die temperature may slowly creep up across cycles to the point that die temperatures and part ejection are too high.

The effect of cooling line depth was examined and it was shown that the bulk die temperature increases with increasing distance between the cavity surface and the line depth. This follows from the principles of conduction but illustration of the temperature patterns made possible with the modelling is quite dramatic.

Intermittent spray, i.e. spray every n^{th} cycle, was shown to be feasible but results in a die that is never in quasi-equilibrium. The bulk die temperature will drift up slightly between spray cycles and drop after the onset of spray.

Illustration of the presence of a dynamic response region close to the die surface and a static region farther from the surface is an example of a result that is extremely useful but not generally understood. One application of this result is assistance in placement of a thermocouple in the die to monitor the consistency of the die temperature from cycle to cycle. The ideal placement level is the transition point between the dynamic and static regions. Placement closer to the surface would result in time-varying data that would be difficult to analyze. Placement deeper than this level would increase the response time delaying detection of temperature shifts.

Die casting is a quasi-equilibrium process at best meaning that ideally the die is in equilibrium cycle to cycle, but not within a cycle. The dynamics of achieving quasi-equilibrium were explored and it was shown that preheating the die to average bulk temperature greatly reduces the time needed to reach cycle to cycle equilibrium (Miller 2016).

Sensitivity studies were performed to examine the effects of die material properties on the thermal response. This was a "what-if" study in the sense that many of the cases studied are not practical and cannot be implemented with current technology, but the results help to explain the limits to better die temperature control. For example, if extremely high conductivity die steels become available, shorter cycles will be possible and die temperatures more uniform, but the heat sinks and the ability to expel heat to the environment will become the new bottle neck.

Perhaps the most significant result of the work was the development of a more complete set of relationships for cooling line performance. Cooling lines, even in simulations, are generally described as a constant temperature heat sink and the heat flux to the line from the die is quantified with a heat transfer coefficient and a temperature differential. In the standard approach, the cooling line diameter and coolant flowrate affect only the heat transfer coefficient. A better Nusselt number correlation for cooling lines was found in the literature and heat exchange design principles were applied to derive design equations that are sensitive to both line diameter and flowrate. The temperature rise in the cooling line as a function of line length and the total heat extraction rate are computed. The temperature rise result provides data useful for comparing expected performance with results on the shop floor.

Technology Transfer and Implementation

Except for the cooling line design work, no new technology resulted from this research. Most of the results are in the form of simple, graphical visualizations of the heat transfer phenomena that occur in die casting dies. The results, particularly the one-dimensional transient and spatial die temperature results, clearly illustrate the effects of cycle time, thermal mass, cooling line placement, etc. NADCA has course materials for both die design and die thermal management that can benefit from the inclusion of explanations in this form. A preliminary revision of course EC 415, Thermal Design and Control, has been completed using results of this work including some of the spatial and transient response examples developed and the new cooling line design relationships. Finalization of the presentation materials and revisions of the text material to include the results of this work will be completed by early 2018.

Much of this work is also relevant to general computer modelling work. Recall that simulations generally do not model cooling lines and quasi-equilibrium is not well understood. Results from this research are included in three new NADCA computer modeling webinars that will be presented for the first time in the fourth quarter of 2017.

Generally modelling results, and especially the quasi-equilibrium results, were presented at the 2016 NADCA Congress and are included in the transactions (Miller 2016).

Acknowledgements

This work was sponsored in part by AMC's *Castings Solutions for Readiness Program*. that is sponsored by the Defense Supply Center Philadelphia, Philadelphia, PA and the Defense Logistics Agency, Ft. Belvoir, VA.

The support of the Defense Logistics Agency and of the NADCA Computer Modeling Task Group is gratefully acknowledged.

In addition, the author extends sincere thanks to Alex Monroe of Mercury Marine for his many comments, suggestions, supplying the production data used for verification, and particularly for his interest in this work. His insights have been most helpful.

References

Gnielinski, V. (1976). "New Equations for Heat and Mass Transfer in Turbulent Pipe and Channel Flow." Int. Chem. Eng. 16: 359-368.

Kakac, S., Y. Yener and A. Pramuanjaroenkij (2014). Convective Heat Transfer, Third Edition. Boca Roton, London, New York, CRC Press, Taylor & Francis Group.

Lienhard V, J. H. and J. H. Lienhard IV (2011). A Heat Transfer Textbook. Mineola, New York, Dover Publications, Inc.

Miller, R. A. (2016). Multi-time Scale Systems and Quasi Equilibrium. 2016 Die Casting Congress and Tabletop. Columbus, OH, NADCA.

Appendix – Heat Transfer to Cooling Lines

A cooling line is a heat exchanger and with a few assumptions can be analyzed with standard techniques common to heat exchanger design (Lienhard V and Lienhard IV 2011). Even though the analysis is straight forward and standard, it is not part of current NADCA courses and text material. Current materials do not consider the fact that the coolant temperature varies through the cooling line. The following derivation results in an improved set of design relationships that are not significantly more complex than those currently used, but are a better representation of the die cooling conditions.

The symbols used in the following discussion are defined in Table 5.

Table 5 Symbols Used in Cooling Line Design

Symbol	Definition
D	Cooling line diameter, m
v	Coolant speed, m/s
Θ	Volumetric flow rate, m^3/s)
μ	Dynamic viscosity, Pa s
ρ	Coolant density of the, kg/m^3
c_p	Coolant specific heat, J/kg °K
h	Heat transfer coefficient, W/m^2 °K
Q	Total heat, J
$\dot{Q}$	Heat transfer rate, W
$\dot{m}$	Mass flow rate, Kg/s
P	Perimeter of the line, m
R_e	Reynolds number, unitless
P_r	Prandtl number, unitless
V	Shot volume, m^3

The volumetric flow rate Θ of the fluid in a circular line is determined by the cross-sectional area of the line and the average speed of the water,

$$\Theta = \frac{\pi \cdot D^2}{4} \cdot v \qquad (1)$$

If the injection temperature is above the liquidus temperature, the total heat that must be dissipated each cycle is the latent heat plus the specific heat of the casting for the temperature range in question, i.e.

$$Q_{Total} = \rho \cdot V \cdot \left(c_p \cdot \left(T_{inject} - T_{eject} \right) + L_f \right) \qquad (2)$$

The heat is extracted from the casting when the die is closed but is dissipated by the die throughout the entire cycle. The total heat removal rate is therefore the total heat divided by the cycle time,

$$\dot{Q}_{Total} = \frac{Q_{Total}}{t_{cycle}} \tag{3}$$

The total heat transfer rate, or a specified proportion of it, represents the total that must be accommodated by the cooling lines. Typical practice is to divide the total heat load into zones and assign a line to each zone. Each line is designed to dissipate the total heat rate from the assigned zone.

Design Relationships

The heat transfer coefficient applicable to cooling lines can be obtained using the appropriate Nusselt number correlation. The so called Dittus-Boelter correlation (Kakac, Yener et al. 2014) has been the correlation of choice for many years but technically it applies only to smooth walled channels and cooling lines are not typically smooth. A better choice, applicable to rough walls and applicable over a wider range of Reynolds numbers is the correlation given in Equation (4) below (Gnielinski 1976, Kakac, Yener et al. 2014).

$$\begin{aligned} N_u &= \frac{(f/2)\cdot(R_e - 1000)\cdot P_r}{1 + 12.7\cdot(f/2)^{1/2}\cdot\left(P_r^{2/3} - 1\right)}; \quad 2300 < \mathrm{R}_e < 10^6, \;\; 0.5 < P_r < 2000 \\ f &= \left(1.58\cdot\ln(R_e) - 3.28\right)^{-2} \end{aligned} \tag{4}$$

The *f* variable in the correlation is a friction factor.

The correlation requires the Reynolds and Prandtl numbers and provides the applicable Nusselt number. The Reynolds, Prandtl, and Nusselt numbers are all dimensionless quantities defined as follows:

$$\mathrm{R_e} = \frac{\rho\cdot D\cdot v}{\mu} = \frac{4\cdot\rho\cdot\Theta}{\mu\cdot\pi\cdot D} \tag{5}$$

$$P_r = \frac{c_p\cdot\mu}{k} \tag{6}$$

$$N_u = \frac{h\cdot D}{k} \Rightarrow h = \frac{k\cdot N_u}{D} \tag{7}$$

Note that the Reynolds number can be equivalently expressed either in terms of linear speed or volumetric flow rate of the coolant. The heat transfer coefficient follows from Equation (7).

The Reynolds number conditions associated with Equation (4) indicate that it applies for flow in the transition and turbulent regions. For lower Reynolds numbers the Nusselt number is constant and typically taken to be (Lienhard V and Lienhard IV 2011),

$$N_u = 4.36, \;\; R_e < 2300 \tag{8}$$

Therefore, depending on the Reynolds number of the coolant flow, the heat transfer coefficient is computed using (7) with the Nusselt number given by either Equation (4) or (8).

Equations for Temperature Change

The basic differential equation that describes the coolant temperature as a function of distance from the inlet, assuming a constant wall temperature, is constructed in terms of the mass flowrate of the coolant. The equation can be equivalently written in terms of the volumetric flow rate. The perimeter is computed from the diameter of the line. The equation is as follows:

$$\frac{d\left(T_{die}-T(x)\right)}{dx}=-\frac{h\cdot P}{c_p\cdot \dot{m}}\left(T_{die}-T(x)\right)=-\frac{\pi\cdot h\cdot D}{c_p\cdot\rho\cdot\Theta}\cdot\left(T_{die}-T(x)\right),\ T(0)=T_{inlet} \tag{9}$$

The solution is a simple exponential function,

$$T_{die}-T(x)=\left(T_{die}-T_{inlet}\right)\cdot e^{-\left(\frac{\pi\cdot h\cdot D}{c_p\cdot\rho\cdot\Theta}\right)\cdot x} \tag{10}$$

Evaluating Equation (9) at the line length L gives the outlet temperature:

$$T_{die}-T_{outlet}=\left(T_{die}-T_{inlet}\right)\cdot e^{-\left(\frac{\pi\cdot h\cdot D}{c_p\cdot\rho\cdot\Theta}\right)\cdot L} \tag{11}$$

Changing the sign and adding $T_{die}-T_{inlet}$ to both sides leads to an expression for the temperature difference across the line,

$$\Delta T=T_{outlet}-T_{inlet}=\left(T_{die}-T_{inlet}\right)\cdot\left(1-e^{-\left(\frac{\pi\cdot h\cdot D}{c_p\cdot\rho\cdot\Theta}\right)\cdot L}\right) \tag{12}$$

An important design relationship follows from Equation (11). The key design parameters are the length, diameter and the flow rate. With a little algebra, Equation (11) reveals these parameters must satisfy

$$\frac{D\cdot L}{\Theta}=-\frac{\rho\cdot c_p}{\pi\cdot h}\cdot\ln\left(\frac{T_{die}-T_{outlet}}{T_{die}-T_{inlet}}\right) \tag{13}$$

Note that the heat transfer coefficient h is a function of the flowrate and the diameter which means that Equation (13) must be solved iteratively.

Heat Transfer Rate

From Newton’s law of cooling, the heat transfer rate from the die to the cooling line over an infinitesimal distance dx is determined by the heat transfer coefficient, the temperature differential between the coolant and the surrounding die, and the infinitesimal area, i.e.

$$\dot{q}=h\cdot\pi\cdot D\cdot\left(T_{die}-T(x)\right)dx \tag{14}$$

The total heat transfer rate for a line of length L is obtained by integrating over the length of the line

$$\dot{Q}=\int_0^L h\cdot\pi\cdot D\cdot\left(T_{die}-T(x)\right)\cdot dx \tag{15}$$

Substituting Equation (10) for the temperature and solving

$$\dot{Q} = c_p \cdot \rho \cdot \Theta \cdot \left(T_{die} - T_{inlet}\right) \cdot \left(1 - e^{-\left(\frac{\pi \cdot h \cdot D}{c_p \cdot \rho \cdot \Theta}\right) \cdot L}\right)$$

Using Equation (12) this simplifies to

$$\dot{Q} = c_p \cdot \rho \cdot \Theta \cdot \left(T_{outlet} - T_{inlet}\right) \tag{16}$$

Equation (16) is unsurprising. The heat transfer rate is the mass flow rate (density times volumetric flow rate) times the temperature change in the mass needed to absorb the indicated amount of heat.